JOURNAL OF Materials CHEMISTRY

A structural study of haematite samples prepared from sulfated goethite precursors: the generation of axial mesoporous voids

Adam S. J. Baker,[a] Adrian S. C. Brown,[a] Martin A. Edwards,[b] Justin S. J. Hargreaves,[a] Christopher J. Kiely,[c] Adrian Meagher[c] and Quentin A. Pankhurst[c]

[a]*Catalysis Research Laboratory, Department of Chemistry & Physics, Nottingham Trent University, Clifton Lane, Nottingham, UK NG11 8NS*
[b]*Materials Science & Engineering, Department of Engineering, University of Liverpool, Liverpool, Merseyside, UK L69 3GH*
[c]*Department of Physics & Astronomy, University College London, Gower Street, London, UK W1CE 6BT*

Received 19th October 1999, Accepted 4th January 2000

A study of the reflection width anisotropy evident in powder X-ray diffraction patterns of haematite prepared from sulfated goethite precursors calcined at low temperatures has been made. HRTEM has shown that the sulfation procedure is responsible for the generation of mesoporous voidage regions which run axially along acicular α-Fe_2O_3 crystals, producing the effects observed in X-ray diffraction. Energy dispersive X-ray elemental mapping has demonstrated the association of such voidage regions with sulfur. Sulfation also inhibits sintering of the haematite crystallites and is associated with an increase in local disorder as evidenced by Mössbauer spectroscopic studies. At higher calcination temperatures the reflection width anisotropy, acicular morphology and porosity is lost. This study indicates that sulfation of goethite may prove a successful and simple route to the synthesis of nanoporous haematite.

Introduction

The preparation of haematite by low temperature calcination of goethite is of technological importance for magnetic storage and catalytic applications.[1] Reflection width anisotropy in the powder X-ray diffraction patterns of such samples, in which non-uniform broadening of the reflections occurs, is well established.[1,2] It is found that the (012), (104), (024), (214) and (018) α-Fe_2O_3 reflections are preferentially broadened with respect to the others. The extent of such differential broadening is strongly dependent upon the calcination temperature used. Under such conditions the morphology of the resultant haematite is known to be acicular, and is a relic of that of the precursor goethite. In the literature a number of possible explanations for the origin of the differential broadening effect have been advanced. Following a careful study of haematite samples of differing morphology using transmission electron microscopy (TEM) and quantitative line profile analysis of powder X-ray diffraction patterns, Duvigneaud and Derie[3] have suggested that the effect is morphological in origin. Since acicular haematite is of markedly anisotropic shape, below a certain critical crystallite dimension the Scherrer crystallite size (and therefore X-ray reflection width) could differ markedly in different directions. Alternatively, it has been proposed by a number of workers [*e.g.* refs. 1, 2] that the effects result from the formation of cationically disordered phases of haematite in which Fe ions are displaced from their equilibrium positions. The goethite to haematite transformation is topotactic, first involving dehydration and then a relocation of cations; the anionic frameworks are structurally similar so relatively little rearrangement of the oxygen lattice is required.[2] In this context, Yamaguchi and Takahashi[4] have argued that there are two sets of reflections. First those which are broad after low temperature heating and whose widths are strongly dependent on the temperature of calcination, and, secondly, those which are narrower and have a lower calcination temperature dependence. The former are generally associated with higher sensitivity to Fe ordering. A third explanation of width anisotropy which has been proposed is related to the development of porosity. The development of well defined porosity during the transformation has been observed in detailed TEM studies.[5–7] Naono and Fujiwara[8] have performed a combined nitrogen adsorption and TEM study and have concluded that the width anisotropy relates to the formation of slit shaped micropores of ≈8 Å diameter running parallel to the needle axes which separate haematite domains of ≈200 Å. On higher temperature calcination, it is argued that sintering occurs forming macropores and the anisotropic effects are consequently lost. In an early single crystal study, Lima de Faria[9] suggested that differential broadening may be the result of the presence of oxygen stacking faults. Reflection satellites which were also observed have been ascribed by others to textural features.[6]

In studies of sulfated haematite catalysts derived from goethite precursors some of the present authors have observed that the sulfation procedure generates similar powder X-ray reflection width anisotropy to that detailed in the studies described above.[10,11] These effects were not evident in analogous non-sulfated samples. No change in gross crystallite morphology on sulfation was observed by TEM, although greater porosity was apparent. Stabilisation of cationic disorder by C_{2v} bridging complexation of SO_4^{2-} to Fe^{3+} in goethite was proposed. In the current study we have further investigated this effect in detail, employing a combination of surface area analysis, transmission electron microscopy, energy dispersive X-ray analysis (EDX), elemental mapping and Mössbauer spectroscopy.

Experimental

Materials preparation

Goethite. 100 ml of a 1 M solution of iron(III) nitrate nonahydrate (Avocado 98+%) prepared using distilled water was added to a Polythene screwtop bottle. To this, 180 ml of a 5 M sodium hydroxide solution was added with stirring. This

solution was then diluted to 500 ml with distilled water and aged in an oven at 70 °C for sixty hours. The resultant yellow precipitate was then filtered off and washed with 4 l distilled water and dried in a vacuum oven for two days. Powder X-ray diffraction confirmed this material to be goethite.

Sulfated haematites. 2 g of goethite were immersed in 30 ml of 0.5 M sulfuric acid for thirty minutes. The solution was then filtered and the filtrate dried at 100 °C overnight. The material was then calcined at the various temperatures specified in static air for three hours.

Haematites. These materials were prepared in an analogous way to their sulfated counterparts, except that immersion was performed in distilled water.

Materials characterisation

Powder X-ray diffraction studies were performed using a Hiltonbrooks modified Philips powder X-ray diffractometer fitted with a detector monochromator. Cu-Kα radiation was used with the X-ray generator operating at 40 kV and 20 mA. Samples were prepared by compaction into an aluminium sample holder and scanned over the range 2θ 5–75° at a step size of 0.05° and counting rate of 2° min^{-1}.

Room temperature ^{57}Fe Mössbauer spectra were collected using a Wissel MA-260S constant acceleration spectrometer. Velocity calibration was performed with respect to α-Fe. A triangular drive waveform was used and the spectra were folded to remove baseline curvature. Measurements were performed on $\approx$50 mg of sample sandwiched between two 2 cm diameter plastic discs.

Samples for TEM examination were gently ground in ethanol using an agate pestle and mortar to produce a fine powder. A drop of the resulting slurry was then allowed to evaporate onto a lacy carbon film supported on a copper mesh grid. These samples were examined using a JEOL 2000FX and a 2000EX High Resolution transmission electron microscope, each operating at 200 kV. Energy dispersive X-ray (EDX) compositional mapping was carried out in a VG HB601 UX STEM equipped with a Link EDX sytem, operating at 100 kV.

Surface area analysis was performed by the Brunauer–Emmett–Teller (BET) method using nitrogen physisorption.

Results and discussion

Series of sulfated and non-sulfated haematites were prepared by calcination of goethite at various temperatures. The surface areas of these materials are given in Table 1. It can be seen that sulfated materials possess BET surface areas roughly twice those of their non-sulfated counterparts. Figs. 1 and 2 show the powder X-ray diffraction patterns of sulfated and non-sulfated materials calcined at 350, 550 and 750 °C. It can clearly be seen that the degree of differential broadening between the different reflections within each diffraction pattern is a function of calcination temperature and is markedly enhanced by sulfation. Additional reflections are evident at 2θ *ca.* 38, 45 and 65°

Table 1 Surface areas of different haematite samples

Sample	Calcination temperature/°C	Surface area/m^2 g^{-1}
H_2SO_4/Fe_2O_3	350	68
	450	58
	550	22
	650	10
	750	5
H_2O/Fe_2O_3	350	38
	450	24
	550	12
	650	5
	750	2

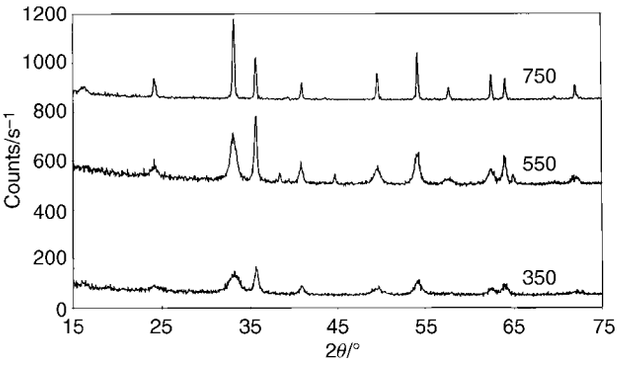

Fig. 1 X-Ray diffraction patterns of haematite prepared from sulfated goethite as a function of calcination temperature, (a) 350, (b) 550 and (c) 750 °C.

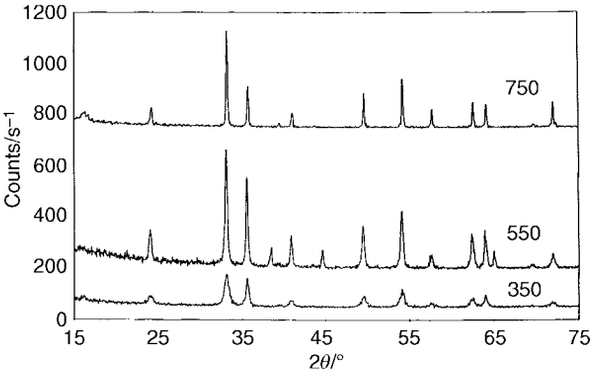

Fig. 2 X-Ray diffraction patterns of haematite prepared from non-sulfated goethite as a function of calcination temperature, (a) 350, (b) 550 and (c) 750 °C.

in the samples calcined at 550 °C. Previously some of the present authors were unable to assign them;[10] however, subsequently, they have been assigned to stray aluminium reflections originating from a sample holder.

Mössbauer spectra of both the sulfated and non-sulfated haematites prepared by calcination at 350 and 550 °C are shown in Fig. 3. All four spectra are dominated by a magnetic sextet with line positions that are close to those of well crystallised haematite. However, unlike well crystallised haematite, the absorption lines are broad, and to varying degrees show asymmetries that are indicative of disordered environments for the iron species, leading to distributions in the local hyperfine parameters experienced at the Fe nuclei. Diamandescu *et al.*[12] have also reported a distribution of hyperfine magnetic sextets in their study of the thermal transformation of goethite into haematite which they attributed to imperfectly crystallised haematite and surface effects. The spectra in Fig. 3 were analysed in terms of a 40 box smoothed probability distribution of hyperfine fields. As a first approximation several simplifying assumptions were made. The isomer shifts and quadrupole splittings of all the subspectra for a given sample were constrained to be equal. The linewidths of the component sextets were set to 0.28 mm s^{-1}, which is an experimental estimate of the natural linewidth. The relative areas of the outer to middle to inner pairs of lines in the sextet were constrained to be 3 : 2 : 1, as appropriate for powder absorbers with no preferential alignment of crystallites. Finally, in addition to a smoothing criterion on the probability distribution, the fits were subject to end point constraints. The results are shown in Fig. 4. The hyperfine field for well crystallised haematite at room temperature is 51.8 T.[1] Fig. 4 verifies that which is apparent from inspection of the spectra, namely (i) the samples that were calcined at 550 °C are less disordered than those calcined at

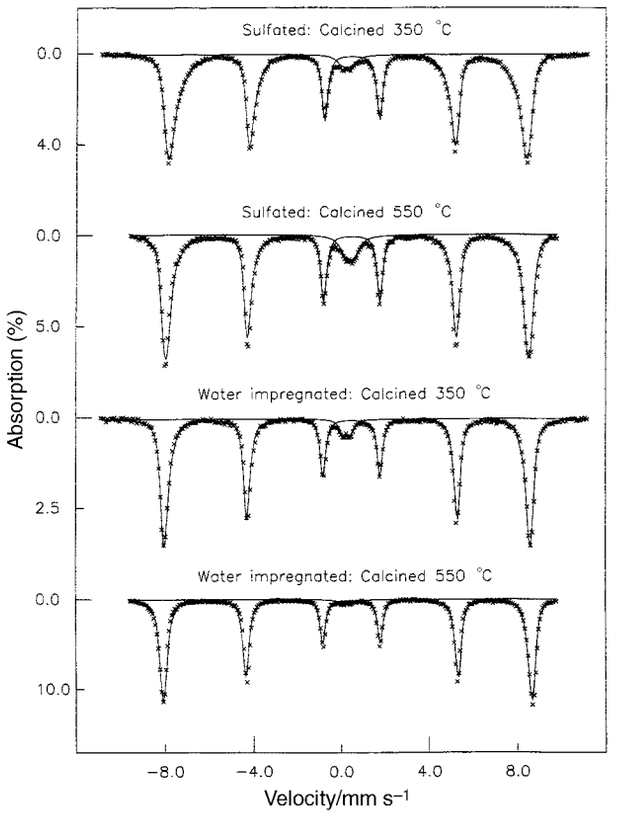

Fig. 3 Mössbauer spectra of haematite prepared *via* different routes.

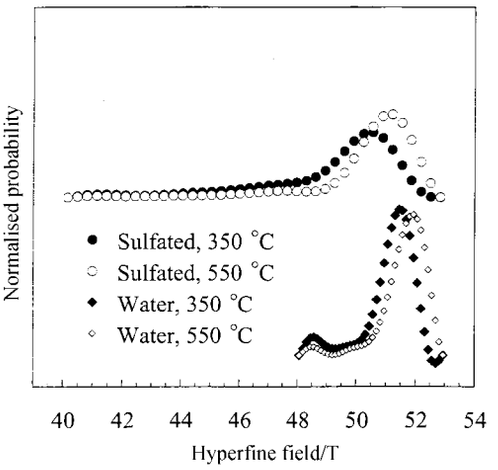

Fig. 4 Hyperfine field distribution of haematites formed by calcination of treated goethites.

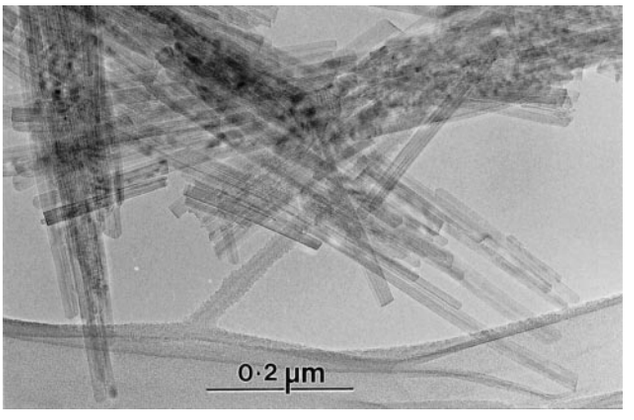

Fig. 5 Bright field electron micrograph of goethite precursor material.

350 °C and (ii) that on calcination the sulfated goethites produce haematites with more disorder than those formed from non-sulfated goethites. The hyperfine field distribution is much closer to that expected for well crystallised haematite in the case of non-sulfated samples. Although it is impossible on the basis of Mössbauer data alone to determine the nature or location of disorder in the different haematite samples, the data obtained are consistent with distributions in the hyperfine field brought about by the presence of S species adjacent to Fe. Given the smooth shapes of the observed hyperfine distributions this may most likely entail interstitial or substitutional defects, rather than a more macroscopic defect structure which would be more likely to give rise to phase separation and the presence of distinguishable sites in the Mössbauer spectra. Finally, there is a small paramagnetic component which appears as a broad singlet or doublet near zero velocity in all the spectra. The most likely explanation is that a fraction of the sample exists in very small crystallites which are undergoing superparamagnetic relaxation at room temperature. The critical dimension of this is of the order of 80 Å for haematite.

Detailed transmission electron microscopy studies have been performed on a selection of the samples: (i) the goethite precursor, (ii) the materials calcined at 350 °C where the observed powder X-ray diffraction width anisotropy is greatest, and (iii) those calcined at 750 °C where the diffraction width anisotropy is at a minimum. Preliminary studies of the samples calcined at 550 °C have been published elsewhere.[10,11]

The goethite precursor material (Fig. 5) displays a characteristic acicular morphology which is consistent with that found in previous studies,[1,8,14] with dimensions of *ca.* 1 μm length (along the [001] crystal direction) and 150 Å width. HREM indicates a high degree of ordering, while the presence of significant porosity was not noted. STEM EDX compositional mapping (Fig. 6) indicates a uniform distribution of S, Fe and O throughout the sulfated precursor material.

The non-sulfated material calcined at 350 °C (Fig. 7(a)) is shown to have an acicular morphology derived from that of the parent goethite, each needle having a [1–10] long axis. Frequently, however, crystallites are observed which are substantially wider in diameter than those of the parent material. These larger crystallites would appear to have been formed by several aligned neighbouring goethite crystallites sintering together during the calcination stage of production. At 623 K the calcination temperature is well above the Huttig Temperature, T_H, for pure α-Fe_2O_3 (where $T_H \approx 0.3T_M$), at which temperature surface species are sufficiently mobile enough to undergo agglomeration and sintering (T_M for α-Fe_2O_3 is 1838 K, thus $T_H^{\alpha\text{-}Fe_2O_3} = 551$ K). The widespread growth of mesopores is evident, being well developed (typically 70 Å in diameter) and distributed throughout the needles. HREM (Fig. 7(b)) shows the material to be well ordered and possess lattice fringe patterns consistent with the Fe_2O_3 structure.

The sulfated haematite calcined at 350 °C (Fig. 8(a)) retains the precursor morphology, although with a slightly decreased needle width of 110 Å. Mesopores are again observed (*ca.* 40 Å diameter), being more prevalent than those in the non-sulfated material. Pore formation commonly occurs along the central axis of needles, often merging to form a single, elongated void running along the entire length of a crystallite, as indicated in Fig. 8(b). HREM imaging (Fig. 8(c)) shows a slightly less well ordered haematite structure although, as with the non-sulfated material, anomalies associated with the stacking faults were not observed within the lattice fringe patterns.

The formation of well defined, regular voidage has previously been observed in studies of the dehydration of goethite by Watari *et al.*[5–7] and Naono and Fujiwara.[8] In the present case it is apparent that the sulfation procedure stabilises the volume fraction of pores and encourages the preservation of smaller voids. STEM EDX compositional mapping (Fig. 9) clearly

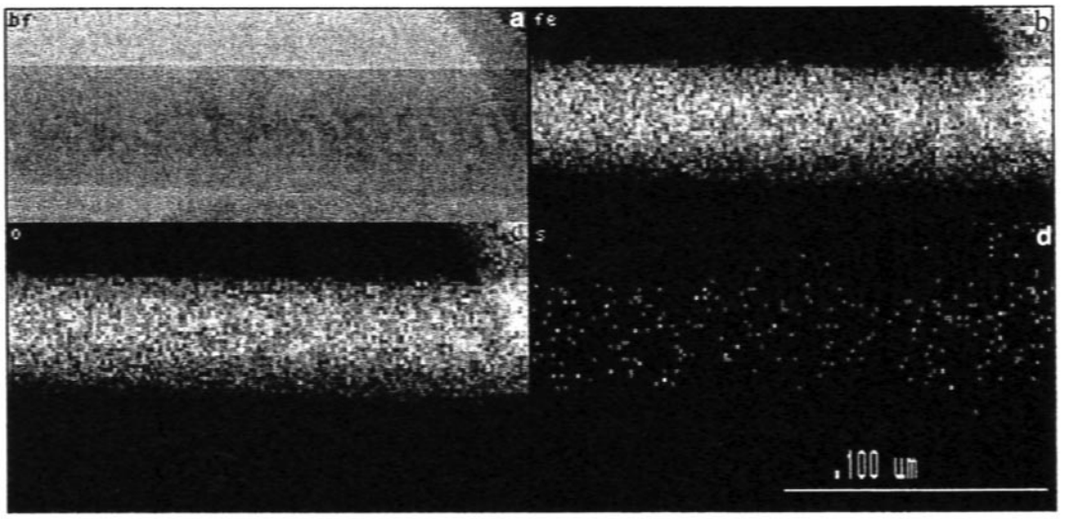

Fig. 6 Elemental mapping of the precursor sulfated goethite.

demonstrates the association of pores with sulfur, with a decrease in concentration of Fe and O due to the corresponding variation in crystalline thickness in these sites. Although protonic acids have been shown to dissolve goethite partially producing holes,[1,13] electron microscopic examination indicates that this is not a major mechanism of pore formation in the present study.

C_{2v} complexation of SO_4^{2-} to goethite has been observed in our FTIR studies of the 550 °C precursor material,[11] where bridging complexation was proposed. The goethite to haematite transformation involves an overall 38% decrease in bulk volume. This is predominantly due to the 25% contraction along the goethite [100] axis associated with the evolution of H_2O.[15] This results in the formation of micropores which are aligned along the crystallite long axis.[8] When calcined at higher temperatures, such as 350 °C in the present case, these voids are able to agglomerate into the observed mesopores. It would appear that such a process is more difficult in the presence of sulfate. SO_4^{2-} ions trapped between the (100) sheets of anions within the goethite matrix segregate to the newly formed voids. As these pores grow and become associated with more SO_4^{2-} groups, the pores become stable and less prone to migration towards the surface of the crystallite. The increased incidence of elongated pores effectively creates a series of internal cylindrical pores running along the centre of the needles which decreases the effective Scherrer crystallite thickness. Related to the above argument, it is interesting that very recently Perez-Maqueda *et al.*[16,17] have made a study of the thermal decomposition of goethite using the controlled rate thermal analysis and concluded that the mobility of surface ions is related to its pore growth and elimination characteristics.

The production or maintenance of internal voids can account for much of the X-ray reflection width anisotropy, although Mössbauer and HREM studies suggest that atomic scale disorder is also a contributing factor. In order to quantify the effects of sulfation on the powder X-ray diffraction patterns, the differences in reflection width between sulfated and non-sulfated samples have been considered as this removes any effects of instrumental broadening. Using the relationship between crystallite thickness and reflection width given by Duvigneaud and Derie[3] for acicular haematite (*i.e.* that the width of the (104) reflection relates to 1.27 × crystal thickness, that for the (116) reflection is 1.35 × the thickness and that for the (024) is 1.89 × crystallite thickness), it is calculated that in the absence of other effects the sulfation procedure reduces the Scherrer crystallite thickness by on average *ca.* 60 Å which compares well to the measured needle "cylinder" wall thickness. Being unaltered, the dimension along the [1–10] needle axis remains the same, hence the relative sharpness of the corresponding (110) reflection is constant. Table 2 lists the full width half maxima used in the calculation which were determined following α_2 stripping using the Rachinger correction. Although the agreement of the TEM and XRD data is close, the Mössbauer and HREM studies previously discussed indicate a contribution of disorder to X-ray reflection widths. Owing to this, and, *e.g.*, the possible influence of instrumental broadening, the overall crystallite dimensions calculated from the diffraction patterns do not exactly coincide with those evidenced by TEM. Additionally, as expected, further calcula-

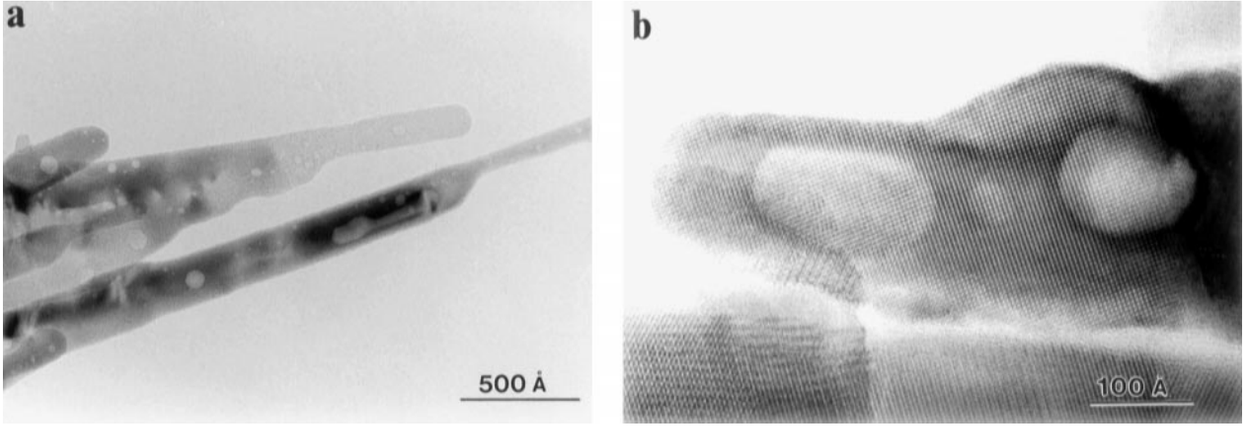

Fig. 7 (a) Bright field electron micrograph, and (b) high resolution micrograph (viewed along the [100] zone axis) of the non-sulfated haematite calcined at 350 °C.

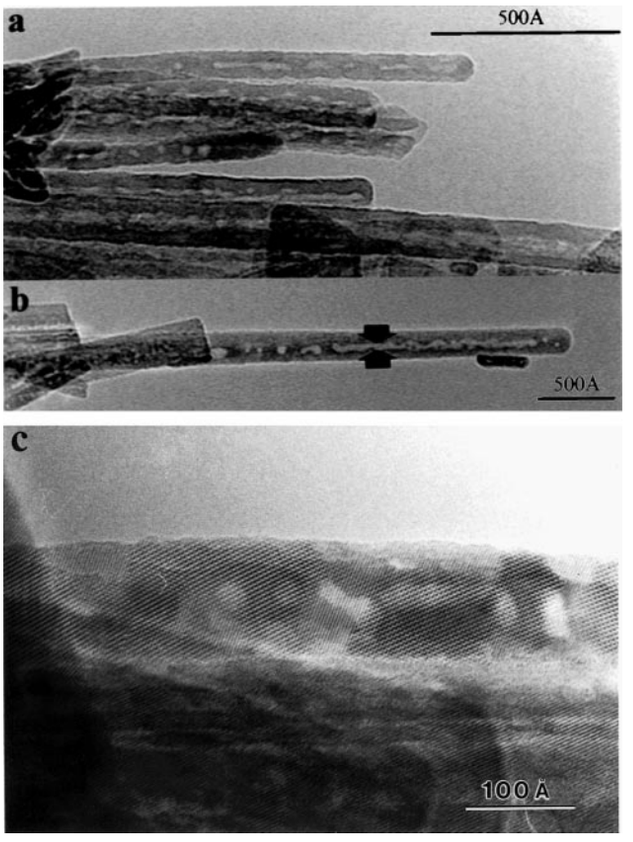

Fig. 8 (a) Bright field electron micrograph (with characteristic elongated cylindrical pores indicated in insert (b)) and (c) high resolution electron micrograph of the sulfated haematite calcined at 350 °C, viewed along the [100] zone axis.

tions show that the surface area differences between the two samples can be accounted for by variations in crystallite size.

The observation of the development of axial mesoporous voids in our materials using the sulfuric acid treatment is likely to be of general interest, since there has been much recent interest in the development of synthetic procedures to produce oxidic materials with regular, well defined mesoporosity, *e.g.* ref. 18. Generally, procedures adopted to date have involved the use of templating, either liquid crystal micellar arrays, *e.g.* ref. 19, or carbon nanotubes,[20] and there have often been associated problems in the complete removal of the template. To our knowledge, it has not proved possible to synthesize

Table 2 Full width half maxima of α_2 subtracted X-ray reflections for haematites calcined at 350 °C

	Full width half maximum/°	
Reflection	H_2O/Fe_2O_3	H_2SO_4/Fe_2O_3
(012)	1.23	2.50
(104)	0.65	1.89
(110)	0.40	0.52
(113)	0.70	0.50
(024)	0.65	1.50
(116)	0.60	1.03
(018)	1.19	[a]
(214)	0.66	1.01
(300)	0.37	0.74
(1010/119)	0.93	[a]

[a]Reflection not discernible above the background.

mesoporous haematite by the above methods. Our observations suggest a potential template free route to these materials, although previous work has shown that sulfation modifies the resultant catalytic properties.[10,11]

The α_2 stripped full width half maxima of samples calcined at 750 °C are given in Table 3. It is evident that there is no differential broadening in these samples although there are slight differences in relative intensity for some reflections between the sulfated and non-sulfated samples. Electron microscopy shows that the acicular morphology has been lost and that crystallites with an ill defined shape have been produced for both the sulfated and non-sulfated samples (Fig. 10(a) and 10(b) respectively). This is consistent with

Table 3 Full width half maxima of α_2 subtracted X-ray reflections for haematites calcined at 750 °C

	Full width half maximum/°	
Reflection	H_2O/Fe_2O_3	H_2SO_4/Fe_2O_3
(012)	0.30	0.35
(104)	0.21	0.26
(110)	0.22	0.26
(113)	0.26	0.21
(024)	0.17	0.25
(116)	0.19	0.20
(018)	0.17	0.24
(214)	0.18	0.19
(300)	0.19	0.19
(1010/119)	0.17	0.20

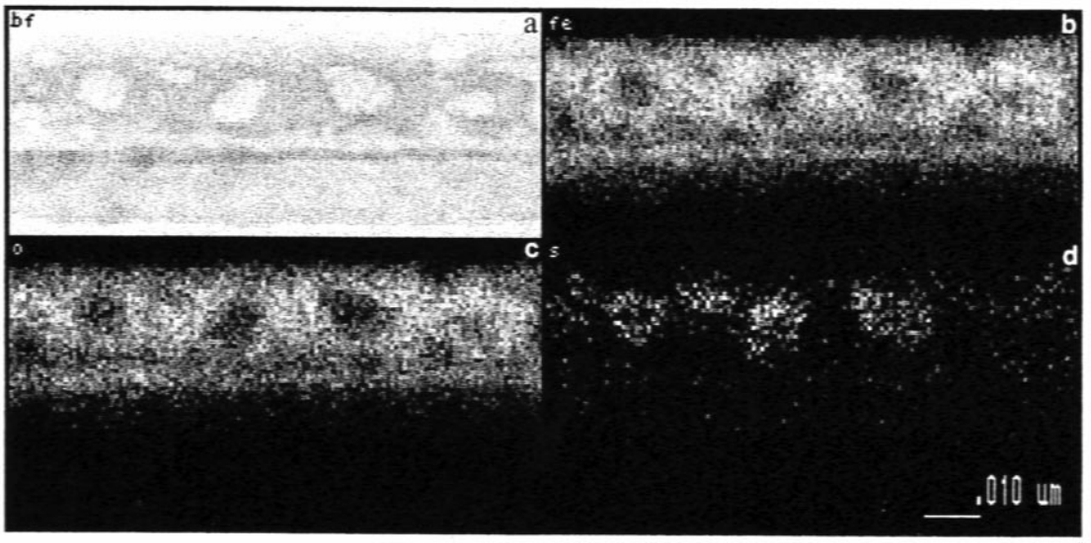

Fig. 9 Elemental mapping of the pore structure of sulfated haematite prepared by calcination at 350 °C.

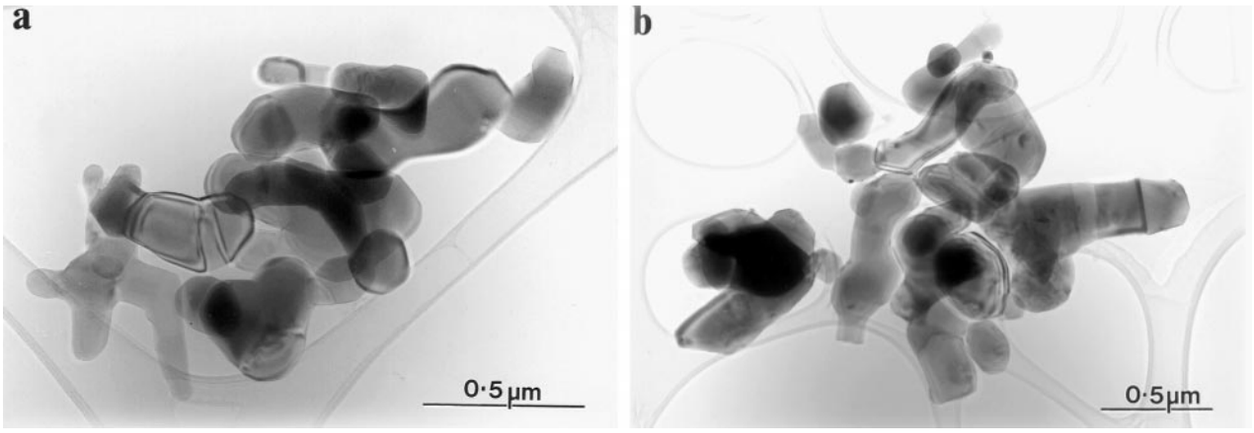

Fig. 10 Bright field electron micrographs of (a) the sulfated haematite and (b) the non-sulfated haematite samples calcined at 750 °C.

previous observations.[1] Additionally, HREM observations show each material to have a well ordered microstructure, with little evidence of porosity. The difference in surface area thus indicates that the non-sulfated samples comprise slightly larger crystallites than their sulfated counterparts. The absence of reflection width anisotropy in materials calcined at higher temperatures can thus be ascribed to the change in crystallite morphology, with associated loss of porosity and an increase in crystallographic ordering. STEM-EDX compositional analysis of the sulfated sample did not show any agglomeration of sulfur to discrete sites. At 1023 K the materials have been calcined at temperatures well in excess of the Tamman temperature ($T_{TAM} \approx 0.5\ T_M$), at which ions are sufficiently mobile for bulk diffusion to occur readily. Pores and any associated sulfur species are thus lost as bulk-to-surface migration becomes possible and the crystallite adopts a more energetically stable structure.

Conclusion

Sulfation of goethite precursors with dilute sulfuric acid prior to low temperature calcination has been shown to enhance anisotropic effects in the powder X-ray diffraction patterns of the resultant haematite which are similar to those previously reported for non-sulfated systems. Transmission electron microscopy studies of haematite samples prepared by the low temperature calcination of goethite demonstrate the maintenance of the acicular morphology of the precursor. Stacking faults are absent and can thus be discounted as a cause of the differential broadening, as can the gross morphology due to the apparently similar needle dimensions between sulfated and non-sulfated samples. However, the sulfation procedure is observed to generate/stabilise the development of well defined porosity and voidage regions in the mesoporous size range. This has the effect of reducing Scherrer crystallite dimensions, and hence increasing reflection widths, in some directions relative to others. Comparison of the features observed in the TEM studies of the materials calcined at 350 °C with those observed in the corresponding powder diffraction patterns demonstrates that this effect is principally responsible for the reflection width anisotropy, although Mössbauer studies also indicate that a degree of cationic disorder may contribute. At higher calcination temperature, where the effects on powder X-ray diffraction patterns are no longer evident, haematite crystallites of irregular morphology and little porosity are produced for both routes.

The results suggest that sulfation of goethite precursors and calcination at low temperature may offer a template-free route to the synthesis of mesoporous haematite.

Acknowledgements

We gratefully acknowledge the kind assistance of Drs. D. E. G. Williams and M. D. Crapper, Department of Physics, University of Loughborough in allowing us to use their powder X-ray diffractometer. The Mössbauer spectra were collected under the auspices of the University of London Intercollegiate Research Service.

References

1 R. M. Cornell and U. Schwertmann, *The Iron Oxides*, VCH Weinheim, 1996.
2 G. Brown, *Associated Minerals*, in *Crystal Structures of Clay Minerals and Their X-ray Identification*, eds. G. W. Brindley and G. Brown, Mineralogical Society, London, 1980, p. 361.
3 P. H. Duvigneaud and R. Derie, *J. Solid State Chem.*, 1980, **34**, 323.
4 T. Yamaguchi and T. Takahashi, *Commun. Am. Ceram. Soc.*, 1982, C83.
5 F. Watari, J. van Landuyt, P. Delavignette and S. Amelinckx, *J. Solid State Chem.*, 1979, **29**, 137.
6 F. Watari, P. Delavignette and S. Amelinckx, *J. Solid State Chem.*, 1979, **29**, 417.
7 F. Watari, P. Delavignette, J. van Landuyt and S. Amelinckx, *J. Solid State Chem.*, 1983, **48**, 49.
8 H. Naono and R. Fujiwara, *J. Colloid Interface Sci.*, 1980, **73**, 406.
9 J. Lima de Faria, *Z. Kristallogr.*, 1963, **119**, 176.
10 A. S. C. Brown, J. S. J. Hargreaves and B. Rijniersce, *Catal. Lett.*, 1998, **53**, 7.
11 A. S. C. Brown, J. S. J. Hargreaves and B. Rijniersce, *Catal. Today*, 1998, **45**, 47.
12 L. Diamandescu, T. Mihaila-Tarabasanu, S. Calgorero, N. Popescu-Pogrion and M. Feder, *Solid State Ionics*, 1997, **101–103**, 591.
13 R. M. Cornell, A. M. Posner and J. P. Quirk, *J. Inorg. Nucl. Chem.*, 1974, **36**, 1937.
14 S. Hirokawa, T. Naito and Y. Yamaguchi, *J. Colloid Interface Sci.*, 1986, **112**, 268.
15 H. Naono, K. Nakai, T. Sueyoshi and H. Yagi, *J. Colloid Interface Sci.*, 1987, **120**, 439.
16 L. A. Perez-Maqueda, J. M. Criado, J. Subrt and C. Real, *Catal. Lett.*, 1999, **60**, 151.
17 L. A. Perez-Maqueda, J. M. Criado, C. Real, J. Subrt and J. Bohacek, *J. Mater. Chem.*, 1999, **9**, 1839.
18 M. J. Hudson and P. A. Knowles, *J. Mater. Chem.*, 1996, **6**, 89.
19 M. E. Spahr, P. Bitterli, R. Nesper, M. Muller, F. Krumeich and H. U. Nissen, *Angew. Chem., Int. Ed.*, 1998, **37**, 1263.
20 C. N. R. Rao, B. Satikumar and A. Govindaraj, *Chem. Commun.*, 1997, 1581.

Paper a908346d